Progr Colloid Polym Sci (2006) 133: 1–8
DOI 10.1007/2882_058

Published online: 19 April 2006

Daoji Gan
L. Andrew Lyon

Amphiphilic, Peptide-Modified Core/Shell Microgels

Daoji Gan
Present address:
E&A Company, Indianapolis, IN, USA

Daoji Gan · L. Andrew Lyon (✉)
Georgia Institute of Technology,
School of Chemistry and Biochemistry,
Atlanta, GA 30332-0400, USA
e-mail: lyon@chemistry.gatech.edu

Abstract Thermoresponsive poly(*N*-isopropylacrylamide) (pNIPAm) core/shell particles bearing primary amine groups in either core or shell were prepared via two-stage, free radical precipitation polymerization, using 2-aminoethyl methacrylate (AEMA) as a comonomer. The amine groups were then used to initiate ring-opening polymerization of γ-benzyl *L*-glutamate *N*-carboxyanhydride (BLG-NCA), producing poly(γ-benzyl L-glutamate) (PBLG) side chains covalently anchored to the particles. Photon Correlation Spectroscopy (PCS) and ^{1}H NMR were employed to characterize these particles. A shift of phase transition to a lower temperature and an increase in particle deswelling volume ratios were observed as a result of grafting hydrophobic PBLG chains to the particles. Further studies by ^{1}H NMR in different solvents indicate that the PBLG chains grafted from the particle shell phase separate on the pNIPAm networks in aqueous media but remain well solvated in DMSO. Together, these results suggest that both core- and shell-grafted architectures can be synthesized with equal ease, and that the particle structure and colloidal behavior can be manipulated by tuning the relative solubility of the network and graft portions of the particle.

Keywords Microgel · Core/shell · PBLG · pNIPAm · Phase separation

Introduction

Considerable research attention has been paid to the stimuli-responsive polymers since they can offer many great potential applications in biomedical fields and in the creation of environmentally responsive materials. Polymers that respond to pH [1], temperature [2], light [3], and protein binding [4] have been reported. Among these polymers, thermosensitive poly(*N*-alkylacrylamides), particularly poly(*N*-isopropylacrylamide) (pNIPAm), have been most widely studied [2, 5–7]. In aqueous media, pNIPAm exhibits a "coil-to-globule" phase transition around 31 °C, which is commonly referred to as a lower critical solution temperature (LCST). This is due to disruption of water-polymer hydrogen bonds and the concomitant hydrophobic association of isopropyl groups. The phase-separating nature of pNIPAm can be exploited to synthesize microgels in the sub-micron size range by precipitation polymerization. Such particles are colloidally stable and possess a sharp volume phase transition (VPT) near the polymer LCST [6]. Furthermore, strong modulation of the physical properties of these particles is observed at the phase transition, including hydrophobicity, porosity, refractive index, colloidal stability, scattering cross section, and electrophoretic mobility. Along with this progress, the particles that have a more advanced architecture have been pursued to generate multifunctional properties. One example of these could be the responsive core/shell or core/corona particles that have been synthesized either to spatially localize the chemical functionalities to the particles [1, 8–11], to render thermoresponsity to non-responsive particles [12, 13],

or to modify a specific physical property of the particles [14].

Previously, we have reported preparation of multiresponsive core-shell particles via incorporation of poly (acrylic acid) into the pNIPAm particles [1]. The particles appeared to be sensitive to both solution temperature and pH. It was also found later that introduction of small amounts of hydrophobic monomer units into the particle shell could significantly change the particle deswelling kinetics without perturbation of the transition thermodynamics [15]. The results suggest that the location of functional groups is very important in the design of responsive colloidal gels. In this contribution, core/shell particles that contain primary amine groups in either the core or the shell were first constructed using the same two-stage polymerizations described previously [1, 9, 11, 15–21]. The amine-bearing particles were then used to initiate another polymerization, producing a hydrophobic polypeptide poly(γ-benzyl L-glutamate) (PBLG) covalently anchored to the desired portion of the particle (Scheme 1). PBLG is an interesting synthetic polypeptide [22] that has been studied in the design of complex colloidal [23] and polymeric structures [24, 25].

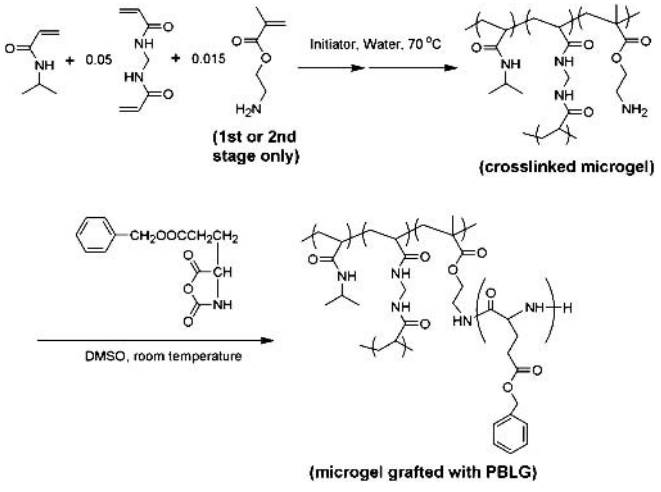

Scheme 1

Experimental Section

Materials

All the chemicals were purchased from Aldrich unless otherwise stated. The monomer *N*-isopropylacrylamide (NIPAm) was recrystallized from hexanes (J.T. Baker) before use. The cross-linker *N*,*N*′-Methylenebis(acrylamide) (BIS), and 2-aminoethyl methacrylate (AEMA), 2,2′-azobis(2-methylpropionamide) dihydrochloride (ABMPAm), and dimethyl sulfoxide (DMSO) were used as received. The amino acid γ-benzyl L-glutamate *N*-carboxyanhydride (BLG-NCA) was synthesized via the reaction of γ-benzyl L-glutamate (BLG) with excess phosgene/benzene solution (Fluka) in dry tetrahydrofuran (THF) at 65 °C; it was purified by crystallization from petroleum ether [22]. Water used in all synthesis and measurements was distilled, and particulate matter was removed via a 0.2 μm filter incorporated into a Barnstead E-Pure system that was operated at a resistance of 18 MΩ.

Synthesis

Low polydispersity pNIPAm microgels were prepared by free-radical precipitation polymerization, using ABMPAm (1 mol % based on the monomer NIPAm) as a cationic initiator and BIS (5 mol %) as a crosslinker. Core/shell microgels were constructed via two-stage polymerization, where the particle core prepared at the first stage served as nuclei in the second-stage polymerization. It should be emphasized that the polymer synthesized in the second stage preferentially precipitates onto the existing seed particles, leading to formation core/shell morphology [1, 8, 16, 26]. Both core particles and core/shell particles were purified via dialysis (Spectra/Pro 7 dialysis membrane, MWCO 10 000, VWR) against water for 14 days, with daily replacement of fresh water. Grafting of poly(γ-benzyl L-glutamate) (PBLG) to the microgels was achieved using primary amine groups incorporated into the particles to initiate ring-opening polymerization of BLG-NCA (Scheme 1). Table 1 lists the chemical compositions and particle size information of microgels used in this study.

Samples C and C–NH_2

To synthesize simple core particles (sample **C**) and amine-modified core particles (sample $C-NH_2$), NIPAm, BIS, and AEMA (1.5 mol % based on NIPAm, Sample $C-NH_2$ only) were dissolved in degassed water with a NIPAm concentration of 0.01 g/mL. The solution was bubbled with nitrogen for 2 h, followed by addition of ABMPAm to start the polymerization. The reaction was then carried out at 70 °C for 6 h.

Sample C/S–NH_2 and C–NH_2/S

To prepare sample C/S–NH_2, NIPAm, BIS, and 1.5 mol % AEMA were introduced to a suspension of sample **C**; the polymer concentration of the dispersion of sample **C** was that which resulted from the initial synthesis of sample **C**. Sample $C-NH_2/S$ was prepared via addition of NIPAm and BIS to a suspension of sample $C-NH_2$. The monomer concentrations used in both shell syntheses were 0.01 g/mL. Both reaction mixtures were nitrogen-bubbled at 70 °C for 2 h. Addition of the ABMPAm triggered the second-stage polymerization, which was then carried out at 70 °C for 6 h.

Table 1 Chemical compositions and particle size information of pNIPAm-based microgels

Sample	Core [a] AEMA, mol-% [b]	*R*, [c] nm	Polyd, % [c]	Shell [a] AEMA, mol-% [b]	Core-shell *R*, [c] nm	Polyd, % [c]	PBLG Grafts Mass, wt % [e]	*R*, [c] nm	*R*, [d] nm
C	0	102	22						
$C/S-NH_2$	0	102	22	1.5	124	23			
C/S-BLG10	0	102	22	1.5	124	23	10	128	112
C/S-BLG20	0	102	22	1.5	124	23	20	135	124
C/S-BLG60	0	102	22	1.5	124	23	60	– [f]	136
$C-NH_2$	1.5	106	20						
$C-NH_2/S$	1.5	106	20	0	125	17			
C-BLG10/S	1.5	106	20	0	125	17	10	120	109
C-BLG20/S	1.5	106	20	0	125	17	20	117	107

[a] Both core and shell were synthesized with BIS (5 mol % based on monomer, NIPAm) as a cross-linker
[b] feed ratio based on NIPAm
[c] Particle radii (*R*) and polydispersity (Polyd.) were measured by PCS at 25 °C in water suspension
[d] radius measured in DMSO at 25 °C
[e] feed ratio of BLG-NCA compared to the microgel used
[f] not measurable due to formation of flocs

Sample C/S-BLG10 and C/S-BLG20

The freeze-dried sample $C/S-NH_2$ (0.07 g) was re-dispersed in 15 mL of DMSO, to which BLG-NCA (10 wt % for **C/S-BLG10**, and 20 wt % for **C/S-BLG20**, based on the $C/S-NH_2$ used) was introduced. The reaction mixture was vigorously stirred at room temperature for 3 days. After this reaction was completed, 15 mL water was added to the solution, and the organic solvent was removed via dialysis against water for 10 days.

Sample C-BLG10/S and C-BLG20/S

To a $C-NH_2/S$ suspension in DMSO, BLG-NCA (10 wt % for **C-BLG10/S**, and 20 wt % for **C-BLG20/S**, based on the $C-NH_2/S$ used) was added, and the grafting reaction was carried out using the same procedure as described above.

Measurements

Photon Correlation Spectroscopy (PCS)

The particle sizes and the size distributions in aqueous solutions were measured by PCS (Protein Solutions, Inc.), with a programmable temperature controller. Prior to taking measurements, the particle solutions were allowed to thermally equilibrate at each temperature for 10 min. Longer equilibration times did not lead to variations in the observed hydrodynamic radii, polydispersities, or scattering intensities. All correlogram analyses were performed with manufacturer-supplied software (Dynamics v.5.25.44, Protein Solutions, Inc.). The data presented below are the averaged values of 20 measurements, with a 15 s integration time for each measurement. The deswelling volume ratios (V/V^*) of the particles were calculated via the relation: $V/V^* = (R/R^*)^3$, where R and R^* are the PCS measured particle radii at the measured temperature and at 25 °C, respectively.

^{1}H NMR

The freeze-dried particles were re-dispersed in either D_2O or DMSO-d_6, and the spectra were then recorded at ambient temperature using a Varian Unity 300 MHz NMR spectrometer. The water peak caused by residual water inside the particles was supressed, in order to more efficiently observe the proton signals of the particles.

Results and Discussion

Synthesis

In these studies, the pNIPAm-based particles were prepared via free radical, precipitation polymerization in aqueous solution at a temperature (70 °C) well above the LCST of pNIPAm. At that temperature, water is a good solvent for the monomer but a poor one for the polymer. Therefore, the growing polymer chains, once reaching a critical length, precipitate from the solution and form stable particles via coagulation of multiple unstable nuclei and by monomer and oligomer capture. A cationic initiator (ABMPAm) renders to the particles positively charged, which is largely responsible for the colloidal stability of the particles. In the synthesis, a crosslinker (BIS) is used to generate polymeric networks, and thus maintain the spherical shape and network connectivity of the particles once

the solution is cooled back to room temperature. To incorporate primary amine groups into the particles, a cationic comonomer (AEMA) bearing a terminal primary amine is copolymerized with NIPAm and BIS.

The core-shell pNIPAm particles were prepared by two-stage polymerization, where the particles prepared at the first stage served as nuclei in the second stage. The oligomers that precipitate from the aqueous solution are preferentially captured by the existing particle cores, which are relatively more hydrophobic and partially deswollen at the reaction temperature [1, 8, 16, 26]. As the polymerization proceeds, the sizes of the existing particles continue to grow, leading to formation of core-shell morphology. Both theoretical prediction and experimental measurements have demonstrated that the total particle number remains constant so that the particle size is only a function of amount of polymer produced at this stage [27, 28]. As such, introducing AEMA at different stages in the polymerization can be employed to locate the amine groups in the particle core or in the shell.

The amine-bearing particles were then used to initiate the ring-opening polymerization of BLG-NCA in DMSO [25], producing PBLG side chains covalently anchored to the particles. Replacement of DMSO with water via dialysis yields a particle/water suspension. Given the much more hydrophobic character of PBLG and higher mobility of these grafted side chains compared to the crosslinked polymer main chains, the grafted PBLG chains are expected to lead to a change in the particle structure and morphology, and thus modulate the physical properties. To investigate the effects of the location of grafted side chains on the particle properties, the PBLG was grafted from either particle core or shell. The chemical compositions and particle size information for these particles are summarized in Table 1.

PBLG Chains Grafted from the Microgel Shell

To investigate the influence of PBLG grafting from a microgel shell, sample $C/S-NH_2$ that contained 1.5 mol % AEMA in the shell was prepared. Shown in Fig. 1 are the PCS measurements of the parent core particles and the core/shell particles as a function of solution temperature. For sample **C**, a simple pNIPAm microgel, the particle sizes gradually decrease with solution temperature until the VPT range (31–36 °C), where a sharply reduced particle size is observed (Fig. 1a). Once the temperature is raised above the volume phase transition temperature (VPTT), the particle sizes do not change with temperature and the curve reaches a plateau. This type of particle size variation has been widely documented as being due to expulsion of water from the particle as pNIPAm becomes insoluble in water at temperatures above the LCST[8]. This temperature induced "coil-to-globule" transition, is a result of disruption of water-polymer hydrogen

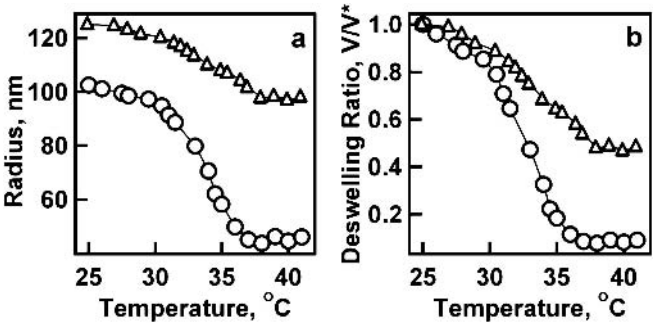

Fig. 1 Hydrodynamic radii (*panel a*) and normalized particle deswelling volume ratios (*panel b*) of samples **C** (*circles*) and $C/S-NH_2$ (*triangles*) as a function of solution temperature

bonds and concomitant formation of hydrophobic associations among isopropyl groups of pNIPAm. Addition of a pNIPAm shell that contains 1.5 mol % AEMA (sample $C/S-NH_2$) leads to a very smooth phase transition (Fig. 1a) with an increased size relative to sample **C** both below and above the pNIPAm LCST.

To directly compare the phase transitions of the core particles and the core-shell particles, the PCS measured particle size variations were normalized to as particle deswelling volume ratios by the calculation method described in Experimental Section. After normalization, these two particles clearly show some difference in the transition behavior (Fig. 1b). Introduction of small amounts of hydrophilic and charged AEMA to the particles results in a broadened transition that apparently shifts to a slightly higher temperature. In addition, the particle deswelling volume ratio in the collapsed state is significantly reduced, i.e. the core/shell particles do not deswell to the same degree as the core particles. These changes in phase transition behavior can reasonably be ascribed to a reduced AEMA-rich phase near the particle periphery. Given the more hydrophilic character of pAEMA compared to pNIPAm, it is reasonable to assume that more pAEMA units would be located at the periphery of the particles due to phase separation during polymerization. Indeed others have combined the techniques of NMR, chemical titration and zeta potential measurements to clearly show the presence of pAEMA-rich phases at the particle periphery in these types of particles [29]. If indeed the outer portion of the shell is largely pAEMA, one would expect an overall decrease in the degree of deswelling, as pAEMA does not display LCST behavior in water and should therefore remain water-swollen even in the presence of a deswollen core.

Shown in Fig. 2 are the PCS measurements of pNIPAm particles shell-grafted with hydrophobic PBLG side chains. For comparison, the measurements of un-grafted particles are also shown in the same figure. Samples **C/S-BLG10** and **C/S-BLG20** are the particles prepared with addition of 10 wt % and 20 wt % of BLG-NCA to sam-

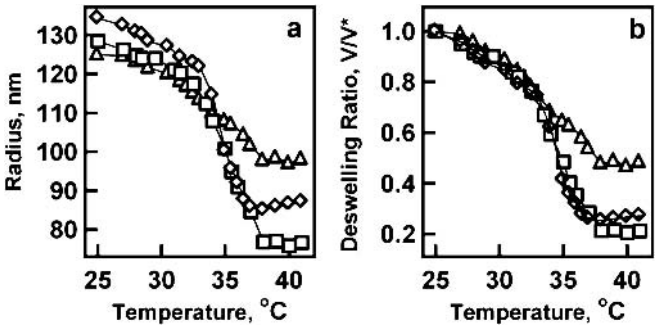

Fig. 2 Dependence of hydrodynamic radii (*panel a*) and particle deswelling volume ratios (*panel b*) on the solution temperature for samples $C/S-NH_2$ (triangles), **C/S-BLG10** (*squares*), and **C/S-BLG20** (*diamonds*)

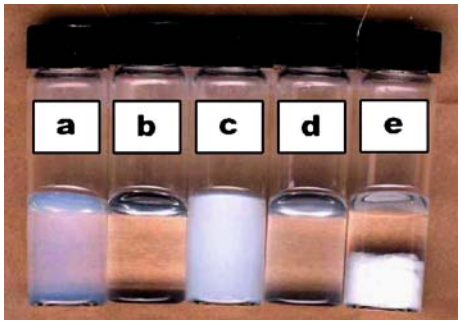

Fig. 3 pNIPAm-based microgels (0.005 g/mL) in different solvents: a, $C/S-NH_2$ in water; b, **C/S-BLG20** in DMSO; c, **C/S-BLG20** in water; d, **C/S-BLG60** in DMSO; e, **C/S-BLG60** in water

ple $C/S-NH_2$. The grafted PBLG chains cause an increase in particle size below the VPTT but a decrease in size above the VPTT relative to the parent core/shell particle (Fig. 2a). Upon normalization as deswelling volume ratios, the difference in the phase transition of those particles can be more easily observed (Fig. 2b). Grafting of PBLG chains to the particles results in a shift of the transition to a lower temperature, and concomitantly an increase in particle deswelling volume ratios in the fully collapse state. This is expected because the hydrophobic PBLG chains were anchored to the particles by amine groups of pAEMA units, which, due to loss of their hydrophilicity and charge, no longer produce a highly swollen particle periphery.

It is interesting to note that **C/S-BLG10** and **C/S-BLG20** have quite similar phase transition behaviors, with the same breadth and sharpness of the transition curves (Fig. 2b). Only a slight difference in the particle deswelling volume ratios is observed in the fully collapsed state. Since these two particles were prepared by the same amounts of initiator (shell-localized amines), it is reasonable to assume that they contain the same number of PBLG chains, and **C/S-BLG20** thus has longer PBLG chains than **C/S-BLG10**. Calculations based on the feed ratios in grafting reactions suggest that the average number of repeat units of PBLG chains are about 20 and 40 for **C/S-BLG10** and **C/S-BLG20**, respectively. In aqueous solution, the hydrophobic PBLG apparently cannot exist as extended chains, and they must fold into a "globule" to minimize contact with water. This effect will be discussed later in the paper in the context of ^{1}H NMR measurements.

Interestingly, longer PBLG chains have a detrimental effect on particle stability in water. Shown in Fig. 3 are representative particles in different solvents. Like pure pNIPAm particles, $C/S-NH_2$ containing 1.5 mol % AEMA in the shell produces a slightly turbid suspension in aqueous media (Fig. 3a) due to slight mismatch of refractive indices between water and the microgels. Sample **C/S-BLG20** is found to be colloidally stable in aqueous media, but the suspension becomes more turbid (Fig. 3c). However, large particle flocs can be seen in Fig. 3e for sample **C/S-BLG60**. In contrast to the particles in water, all particle suspensions in DMSO, including $C/S-NH_2$ (not shown) appear completely transparent, regardless of the grafted PBLG content (Fig. 3b and 3d). It should be emphasized that even though **C/S-BLG60** precipitates completely in water (Fig. 3e), it still produces very stable microgels without any precipitates in DMSO (Fig. 3d). PCS measurements indicate that **C/S-BLG60** exists as monodispersed, colloidal particles in DMSO, with an average particle size larger than that of **C/S-BLG10** and **C/S-BLG20** (Table 1). The flocculation of **C/S-BLG60** in water can be explained as formation of inter-particle hydrophobic association driven by the higher average molecular weight of the grafted PBLG chains. Obviously, this is not the case in DMSO since both pNIPAm and PBLG have good solubility in this solvent.

To further investigate the structure of the particles, ^{1}H NMR experiments were performed after re-dispersing the freeze-dried sample into deuterated solvents. Shown in Fig. 4 are representative NMR spectra of **C/S-BLG20** in two different solvents, DMSO-d_6 and D_2O. DMSO is a good solvent for both pNIPAm and PBLG segments, while we expect D_2O to be a good solvent only for the pNIPAm portion of the microgels. The characteristic proton signals of isopropyl groups from pNIPAm units are observed as Peak **a** and **b**, which can be assigned to the methyl and methylene protons, respectively. Peak **f** at 5.0 ppm is contributed by the α-methylene protons of benzyl groups from PBLG segments, whose aromatic proton signals are located at 7.1–7.5 ppm (Peak **e**). The proton signal **i** from PBLG is buried under a large peak arising from the complex formed between DMSO and residual H_2O. The proton signals **c** and **d**, contributed from polymer backbone of the particles, overlap with signal **h** and **g** of PBLG. In all, the proton assignments are consistent with the chemical structure of the polymer.

Inspection of the NMR spectrum suggests that Peak **b** and **f**, exclusively contributed from pNIPAm and PBLG, respectively, are well resolved. Therefore, taking the ratio

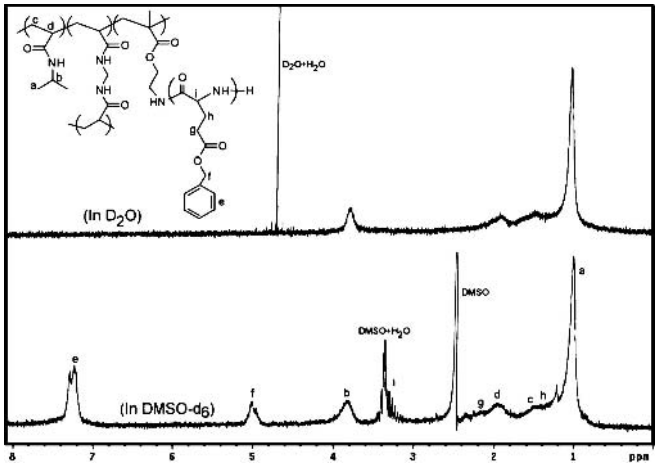

Fig. 4 ^{1}H NMR spectra of sample **C/S-BLG20** in D_2O and DMSO-d_6. The grafted PBLG side chains cannot be detected in D_2O due to phase separation

of integrated areas of these two peaks should give some information about the chemical compositions of the particles. It is surprising to find that the PBLG content observed by NMR technique is approximately two times that which is calculated from the feed ratio used in the reaction. The same phenomenon was observed for **C/S-BLG10** (about 1.5 times apparent excess). In a striking contrast, the ^{1}H NMR spectrum recorded in D_2O, which is a good solvent for pNIPAm but a poor one for PBLG, only shows the signals of pNIPAm segments with the PBLG resonances being completely absent from the spectrum.

Based on these results, a morphological description is proposed to explain the possible behavior of PBLG chains anchored to the pNIPAm particle shell. Water is a good solvent for pNIPAm (at ambient temperature) but a non-solvent for PBLG. In aqueous media, the PBLG chains may thus be forced to phase separate into a globular conformation on or inside the microgel, leading to disappearance of the proton signals of PBLG in D_2O. This phenomenon is quite similar to the widely reported micelle formation by amphiphilic block copolymers, where the hydrophobic blocks form the core and the hydrophilic ones form the shell of the micelle in aqueous media [30–32].

By comparison, DMSO is a good solvent for both PBLG and pNIPAm, thereby allowing the PBLG side chains to adopt a solvated chain conformation. The apparently higher PBLG content observed by NMR in DMSO-d_6 may arise from the inherent heterogeneity of the microgel particles. The particle core becomes compressed after shell addition and has a denser network structure [18–20]. Therefore the relaxation time of some pNIPAm units inside the particles may be too short to be detected by NMR. In contrast, the grafted PBLG chains located at the particle shell have large mobility, thus the relaxation time is long enough to be followed by the NMR techniques.

PBLG Grafted from the Microgel Core

Given the inherent porosity of microgels, we examined the feasibility of grafting PBLG chains from particle core. For this purpose, another type of core/shell particle, $C-NH_2/S$, was synthesized such that the particle core contained 1.5 mol % AEMA, while the shell was composed of pNIPAm. The temperature dependence of the particle sizes is shown in Fig. 5 for the core particles and the core/shell particles. The core particles display an elevated VPTT and a relatively small degree of deswelling, presumably due to the presence of the cationic monomer. Compared to the core particles, the core/shell particles have increased sizes in both the fully collapsed and swollen state (Fig. 5a). Furthermore, addition of pure pNIPAm shell layer diminishes the function of the hydrophilic AEMA located in the core since the particle shell plays a dominant role in the transition behavior as described in previous publications [18–20]. As a result, the core-shell particles collapse at a lower temperature than the core particles The differences in swelling behavior can be more easily observed when the particle size variations are normalized to deswelling volume ratios (Fig. 5b). Apparently, after addition of pure pNIPAm shell around the AEMA-containing core, the phase transition becomes sharper and shifts to a lower temperature. Along with those changes is a decrease in the deswelling volume ratios at fully collapsed state. All these results are consistent with those of $C/S-NH_2$ discussed above.

^{1}H NMR analysis was performed to determine the chemical compositions of the particles, and thus to evaluate the efficiency of the PBLG grafting to the particles containing amine groups in the core (Fig. 6). The ungrafted particles, $C-NH_2/S$, show proton signals mainly contributed from pNIPAm units, as well as peaks due to DMSO and $DMSO/H_2O$ complex. It is worth mentioning that a broad peak at 7.0–7.6 ppm can be assigned to amide groups of pNIPAm. This signal cannot be detected in D_2O, because exchange of amide protons with D_2O is so fast that the signal is buried in the HDO resonance [33]. Sam-

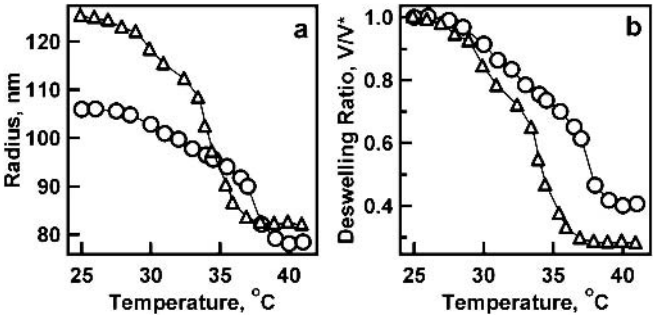

Fig. 5 Variations of hydrodynamic radii (*panel a*) and normalized particle deswelling volume ratios (*panel b*) with solution temperature for sample $C-NH_2$ (*circles*) and $C-NH_2/S$ (*triangles*)

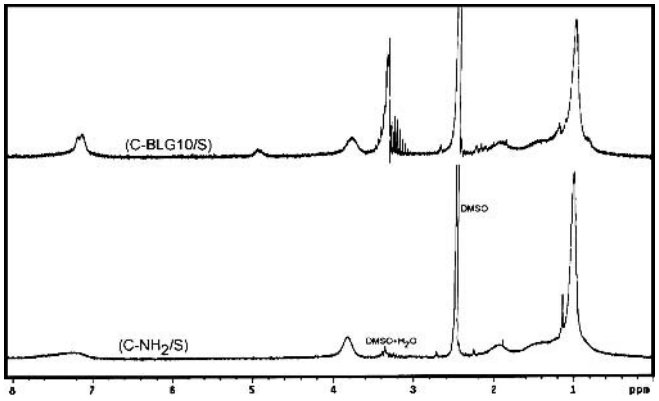

Fig. 6 ^{1}H NMR spectra of samples $C-NH_2/S$ and **C-BLG10/S** in DMSO-d_6

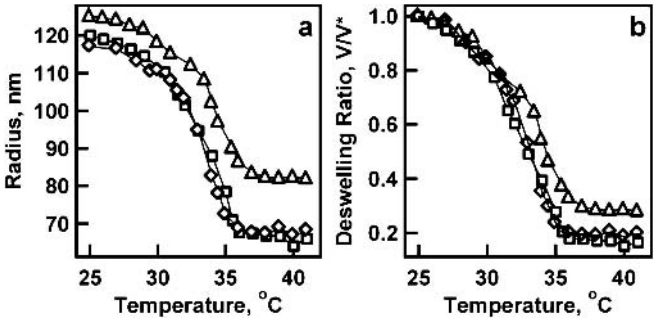

Fig. 7 Hydrodynamic radii (*panel a*) and normalized particle deswelling volume ratios (*panel b*) of sample $C-NH_2/S$ (*triangles*), **C-BLG10/S** (*squares*), and **C-BLG20/S** (*diamonds*) as a function of solution temperature

ple **C-BLG10/S** displayes the signature peaks of PBLG chains centered at 5.0 and 7.3 ppm, indicating a successful grafting of PBLG chains from the pNIPAm-AEMA core. The calculation of NMR integration ratios, as described above, shows that the grafted PBLG contents are very close to those used in the momomer feed. Given the previous observation of higher than expected PBLG content for the shell-grafted microgels, it is apparently the case that the core is less compressed and/or the PBLG is more restricted in the core-grafted case, thereby leading to an apparent peak integration that is closer to the predicted value.

The effects of grafting PBLG chains on the phase transition of the particles can be seen from Fig. 7, which shows the PCS measured particle size variations as a function of solution temperature. Here **C-BLG10/S** and **C-BLG20/S** denote particles with 10 and 20 wt %, respectively, of PBLG grafted to the $C-NH_2/S$ particles. Contrary to what was observed for the shell-grafted microgels, **C-BLG10/S** and **C-BLG20/S** have reduced sizes in the swollen and condensed state in comparison to the ungrafted $C-NH_2/S$ (Fig. 7a). These results may suggest that the increased hydrophobicity brought about by grafting PBLG into the particle core decrease the equilbrium swelling volume below the VPTT, as well as a decreased water content in the condensed state.

On the other hand, there are some similarities for the particles with PBLG grafted from either the core or the shell, which can be seen from the normalized particle deswelling volume ratios as shown in Fig. 7b. Again, as a result of grafting PBLG chains to the particles, a relatively sharp phase transition that also shifts to a lower temperature is observed accompanying with an increase in the particle deswelling volume ratios in the fully collapsed state. These results can be ascribed to termination of hydrophilic AEMA units by hydrophobic PBLG chains.

Conclusions

It has been demonstrated that hydrophobic PBLG chains can be grafted to the pNIPAm particles from either the core or the shell, using particles bearing primary amine groups to initiate ring-opening polymerization of BLG-NCA. As a result of termination of these charged hydrophilic groups in the particles, the phase transition of the particles becomes sharper and shifts to lower temperature, while the particle deswelling volume ratios increase. In aqueous media, the PBLG grafted from particle shell exists as phase separated globules on the particle surface. Surprisingly, for low degrees of polymerization (< 40 monomer units) the shell-grafted PBLG microgels are colloidally stable in water, despite the relative hydrophobicity of the shell. However, longer chains with presumably more conformational flexibility, lead to particle flocculation in water due to interparticle PBLG association.

Acknowledgement LAL acknowledges support from the National Science Foundation Division of Materials Research under Grant No. 0203707.

References

1. Jones CD, Lyon LA (2000) Macromolecules 33:8301
2. Schild HG (1992) Prog Polym Sci 17:163
3. Kungwatchakun D, Irie M (1988) Makromol Chem-Rapid 9:243
4. Kim J, Nayak S, Lyon LA (2005) J Am Chem Soc 127:9588
5. Heskins M, Guillet JE (1968) J Macromol Sci Chem A2:1441
6. Pelton R (2000) Adv Colloid Interface Sci 85:1
7. Saunders BR, Vincent B (1999) Adv Colloid Interface Sci 80:1
8. Berndt I, Pedersen JS, Richtering W (2005) J Am Chem Soc 127:9372
9. Nayak S, Lee H, Chmielewski J, Lyon LA (2004) J Am Chem Soc 126:10258

10. Nayak S, Lyon LA (2004) Angew Chem Int Ed Engl 43:6706
11. Nayak S, Gan D, Serpe MJ, Lyon LA (2005) Small 1:416
12. Makino K, Yamamoto S, Fujimoto K, Kawaguchi H, Ohshima H (1994) J Colloid Interface Sci 166:251
13. Senff H, Richtering W, Norhausen C, Weiss A, Ballauff M (1999) Langmuir 15:102
14. Shiroya T, Tamura N, Yasui M, Fujimoto K, Kawaguchi H (1995) Colloid Surf B-Biointerfaces 4:267
15. Gan D, Lyon LA (2001) J Am Chem Soc 123:7511
16. Gan D, Lyon LA (2001) J Am Chem Soc 123:8203
17. Gan D, Lyon LA (2002) Macromolecules 35:9634
18. Jones CD, Lyon LA (2003) Macromolecules 36:1988
19. Jones CD, Lyon LA (2003) Langmuir 19:4544
20. Jones CD, McGrath JG, Lyon LA (2004) J Phys Chem B 108:12652
21. Nayak S, Lyon LA (2004) Angew Chem 116:6874
22. Fuller WD, Verlander MS, Goodman M (1976) Biopolymers 15:
23. Fong B, Russo PS (1999) Langmuir 15:4421
24. Schmidtke S, Russo P, Nakamatsu J, Buyuktanir E, Turfan B, Temyanko E, Negulescu I (2000) Macromolecules 33:4427
25. Block H (1983) Poly(gama-benzyl-L-glutamate) and other glutamic acid containing polymers. New York
26. Berndt I, Richtering W (2003) Macromolecules 36:8780
27. Marion P, Beinert G, Juhue D, Lang J (1997) Macromolecules 30:123
28. Kawaguchi S, Winnik MA, Ito K (1995) Macromolecules 28:1159
29. Meunier F, Elaissari A, Pichot C (1995) Polym Adv Technol 6:489
30. Thurmond KB II, Kowalewski T, Wooley KL (1996) J Am Chem Soc 118:7239
31. Inoue T, Chen G, Nakamae K, Hoffman AS (1998) J Controlled Release 51:221
32. Zhao Y, Liang H, Wang S, Wu C (2001) J Phys Chem B 105:848
33. Larsson A, Kuckling D, Schonhoff M (2001) Colloids Surf A 190:185